Polarization-enhanced absorption spectroscopy for laser stabilization

Paul D. Kunz,[1,2,*] Thomas P. Heavner,[1] and Steven R. Jefferts[1]

[1]Time and Frequency Division, National Institute of Standards and Technology, Boulder, Colorado 80305, USA

[2]Department of Physics, University of Colorado, Boulder, Colorado 80309, USA

*Corresponding author: kunzp@nist.gov

We demonstrate a variation of pump-probe spectroscopy that is particularly useful for laser frequency stabilization. The polarization-enhanced absorption spectroscopy (POLEAS) signal provides a significant improvement in signal-to-noise ratio over saturated absorption spectroscopy (SAS) for the important and commonly used atomic cycling transitions. The improvements can directly increase the short-term stability of a laser frequency lock, given sufficient servo loop bandwidth. The long-term stability of the POLEAS method, which is limited by environmental sensitivities, is comparable to that of SAS. The POLEAS signal is automatically Doppler-free, without requiring a separate Doppler subtraction beam, and lends itself to straightforward compact packaging. Finally, by increasing the amplitude of the desired (cycling) peak, while reducing the amplitude of all other peaks in the manifold, the POLEAS method eases the implementation of laser auto-locking schemes.

OCIS codes: (300.6360) Spectroscopy, laser; (140.3425) Laser stabilization; (300.6170) Spectra; (300.1030) Absorption; (000.2170) Equipment and techniques.

http://dx.doi.org/10.1364/AO.52.008048

1. Introduction

Numerous methods exist for frequency-stabilizing a laser, including various cavity-based approaches, which hold the record for short-term stability [1], and spectroscopy-based approaches [2], which provide longer-term stability. Here, we present a spectroscopy-based laser stabilization method that we call polarization enhanced absorption spectroscopy (POLEAS). This method is related to two other commonly used methods, Doppler-free saturated absorption spectroscopy (D-F SAS) [3,4] and polarization spectroscopy (PS) [5–12]. The POLEAS method combines some of the favorable aspects from both D-F SAS and PS, resulting in a more stable, robust, and compact laser frequency lock. The unique combination of features offered by POLEAS makes it a superior candidate for many applications requiring laser frequency stabilization.

When comparing the three Doppler-free, nonlinear spectroscopy methods, POLEAS, D-F SAS, and PS, there are general commonalities; however, there are also important differences in the details of what each method offers to laser-locking applications. They each reveal narrow (<10 MHz), non-Doppler-broadened hyperfine spectrum features, due to the velocity-selective, counter-propagating beam configuration that they have in common. They also each use balanced photodetectors (circuits that output the difference between the signals detected by two separate photodiodes), which results in the cancellation of the Doppler-broadened background profiles. One important difference between them is that the POLEAS and D-F SAS output signals consist of resonant absorption or transmission *peaks*, whereas the PS signal consists of *dispersion-shaped* curves at the atomic resonant frequencies. The PS dispersion signals of some atomic transitions (in particular, closed

or cycling transitions), are suitable for directly stabilizing a laser to the atomic resonance. On the other hand, locking a laser to the top of an absorption peak (as with D-F SAS and POLEAS) requires an additional stage of modulation to generate an error signal. This error signal is generally achieved through phase-sensitive demodulation electronics, whereby the signal is modulated and then demodulated, yielding the derivative of the absorption peak. While this phase-sensitive detection requires specialized electronic equipment that can be costly and cumbersome, it provides the distinct advantage of being relatively insensitive to changes in the signal amplitude (e.g., due to temperature fluctuations or laser intensity). The frequency stability of D-F SAS, afforded by its narrow peaks and associated phase-sensitive detection, largely accounts for its widespread use in laser stabilization applications.

In this paper, we describe the POLEAS signal and its relative merits when compared with D-F SAS and PS. We show the simple and compact apparatus needed to realize the POLEAS method. We report on its reliable performance when used to stabilize laser frequencies for atomic laser-cooling experiments. Finally, we address environmental sensitivities of the various spectrometers, and discuss measurements that indicate their relative long-term stabilities.

2. Spectroscopy Signal

Both PS and POLEAS rely on the effects that polarized atoms have on a probe beam. An atomic vapor can be polarized using a circularly polarized pump beam. The polarized vapor has different electric susceptibilities, χ_+ and χ_-, for right- and left-handed circularly polarized probe light. These complex electric susceptibilities can be decomposed into their real and imaginary parts; the imaginary parts yield absorption coefficients, α_+ and α_-, and the real parts correspond to indices of refraction, n_+ and n_-. By using a linearly polarized probe beam (i.e., an equal mixture of right- and left-hand circular polarization) the differences, $\Delta\alpha = \alpha_+ - \alpha_-$ and $\Delta n = n_+ - n_-$, can result in clear spectroscopy signals. The refraction difference Δn rotates the plane of optical polarization and is referred to as gyrotropic birefringence. The PS method detects this polarization rotation of the probe light induced by the birefringence of Δn. On the other hand, the absorption difference $\Delta\alpha$ makes the probe beam elliptically polarized (by scattering more of one circular polarization than the other). The POLEAS scheme detects this ellipticity of the probe light, induced by the absorption difference $\Delta\alpha$.

The detectors used in the PS and POLEAS schemes to observe the effects of Δn and $\Delta\alpha$, respectively, closely resemble each other. A *balanced polarimeter* is used, in the case of PS, to detect the rotation of the plane of polarization. The balanced polarimeter usually consists of a half-wave plate, a polarizing beam splitter (PBS), and a balanced photodetector. The half-wave plate rotates the

polarization axis of the light to 45 deg, relative to the axis of the PBS [6,7]. In this way, the difference in power at the two detectors is correlated with a polarization rotation from the atomic vapor. Correspondingly, a *circular analyzer* (see Fig. 2) is used, in the case of POLEAS, to detect the ellipticity of the polarization. This circular analyzer is implemented by replacing the half-wave plate in the balanced polarimeter with a quarter-wave plate. When the quarter-wave plate is at 45 deg, the two circular polarization components are projected onto the horizontal and vertical axes of the PBS. The PBS then separates these two components and directs them onto the balanced photodetector. Note that it is possible to achieve either the balanced polarimeter or the circular analyzer by use of the same optical components by adjusting the various rotation orientations, as pointed out by Yashchuk *et al.* in the context of magneto-optical spectroscopy [13].

3. Theoretical Model

There are many reports in the literature regarding the theoretical modeling of D-F SAS and PS (see [14–18] and the references therein), and much of that work can be directly adapted to the present POLEAS case. In particular, Noh *et al.* [14] have developed a detailed analytical model, with tabulated results, that can be readily applied to a variety of pump-probe spectroscopy schemes, including D-F SAS, PS, and POLEAS. Their model can discriminate between the effects of optical pumping and saturation, and can be used to predict the dependence of the signal on beam diameter and intensity [15].

The calculations proceed in the following way: the rate equations for all the relevant atomic transitions are derived and then solved to obtain the level populations [16]. These level populations are then used to solve for the electric susceptibility [17]. This requires integrating over the Maxwell–Boltzman velocity distribution, which, when carried out, yields functions whose imaginary (real) parts are Lorentzian (dispersive). The dispersive functions, from the real part of the susceptibility, correspond to the birefringence and hence to the signals obtained with PS [18]. The Lorentzians, from the imaginary part of the susceptibility, correspond to the absorption coefficients and, thus, to the signals obtained with D-F SAS [15,19] and POLEAS.

We have used the developed theoretical models to predict the POLEAS signal for the $5S_{1/2} F = 2 \rightarrow 5P_{3/2}$ $F' = 1$, 2, and 3 transitions of ^{87}Rb atoms. In Fig. 1(a), we show the relevant energy level diagram of atoms optically pumped by the σ^+ pump beam. The allowed $\sigma^\pm$ probe transitions and their relative strengths are also represented. Figure 1(b) shows both the two individual signals detected by the arms of the circular analyzer (the Doppler-broadened background has been omitted and the signals offset vertically for clarity), and the full POLEAS output resulting from the difference between the two individual signals.
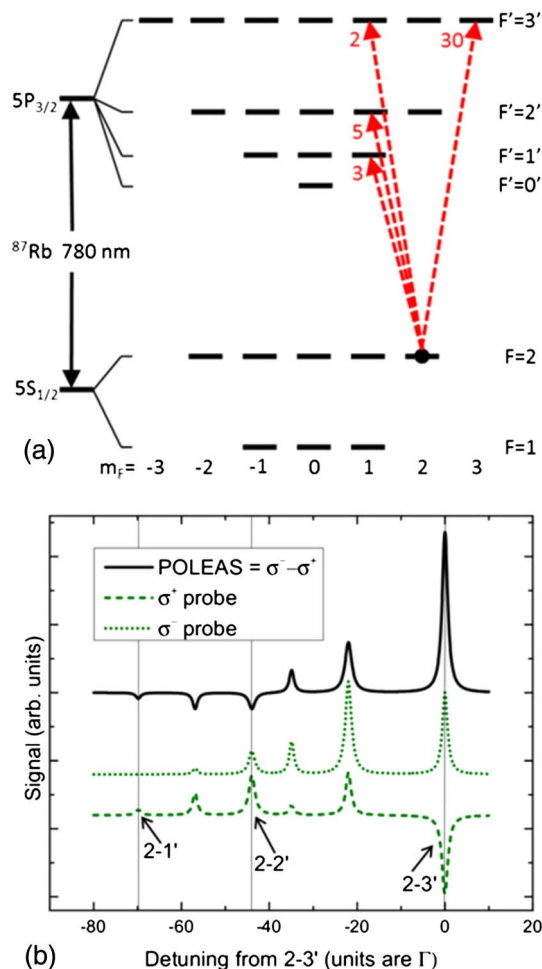
Fig. 1. (a) ^{87}Rb D2 level diagram (not to scale) showing population optically pumped by σ^+-polarized light to the $|2, 2\rangle$ state. The numbers and dashed arrows show the allowed $\sigma^\pm$ transitions and their relative strengths. (b) Predicted spectra of the POLEAS apparatus. The dashed lines are the individual signals (with Doppler backgrounds removed and vertically offset for clarity) that would be detected by the two arms of the circular analyzer, and the solid line is the full POLEAS output signal of the ^{87}Rb D2 $F = 2 \rightarrow F'$ manifold. Frequency units are natural linewidths ($\Gamma = 2\pi\, 6$ MHz).

The resonance features of the individual signals are all positive peaks except for the $F = 2 \rightarrow F' = 3\ \sigma^+$ resonance, which is a negative peak. The dominant mechanism behind these features is optical pumping, both between Zeeman sublevels and hyperfine states [4,14,20]. Hyperfine depopulation pumping is effective in the majority of transitions and is largely responsible for the increased transmission, resulting in positive peaks. In the case of the $F = 2 \rightarrow F' = 3\ \sigma^+$ transition, hyperfine depopulation pumping is ineffective due to the transition's closed cycling nature (i.e., there is no direct dipole-allowed decay path to the dark $F = 1$ hyperfine state from $|3, 3\rangle$). Pumping among the Zeeman sublevels causes population to build up in the $|2, 2\rangle$ stretched ground state sublevel (i.e., the atoms become polarized). The σ^+ probe beam absorption is thus enhanced, resulting in a negative peak.

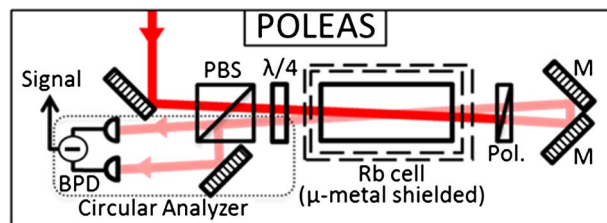
Fig. 2. POLEAS apparatus. PBS, polarizing beam splitter; $\lambda/4$, quarter-wave plate; Pol, polarizer; M, mirror; BPD, balanced photodetector.

4. Apparatus

The experiments described in this paper use the following laser configuration: a 780 nm distributed-Bragg-reflector (DBR) diode laser beam is collimated, sent through a 60 dB optical isolator, and coupled into a single-mode polarization-maintaining fiber. The laser has a full width at half-maximum (FWHM) free-running linewidth of 1 MHz at 1 s measurement time. The fiber output collimator yields a Gaussian beam of $1/e^2$ diameter 7.5 mm. Immediately after the output collimator is a PBS, configured so that the optical power coming out of the two PBS ports is divided equally (i.e., half S polarized and half P polarized). Irises and neutral density filters are subsequently used to control the size and power of each output beam. One beam is sent to a standard D-F SAS configuration [3], and the other beam is sent to the POLEAS configuration.

The POLEAS apparatus is diagrammed in Fig. 2. An input beam passes through a linear polarizer (we use the S port of a PBS, as shown in Fig. 2), and then a zero-order quarter-wave plate to obtain the circularly polarized pump beam. This circularly polarized pump beam then passes through a pyrex, 7.2 cm long, room temperature, rubidium vapor cell. The vapor cell is magnetically shielded by μ-metal, such that the magnetic fields are reduced to below 2 mG in the transverse direction, and below 10 mG in the longitudinal direction. Following the vapor cell is another polarizer, which not only linearizes the polarization, but also reduces the power, yielding the desired probe beam. This probe beam is nearly retro-reflected upon itself by mirrors, but the mirrors are angled just enough that the probe beam can be spatially separated from the incoming pump beam. The passage of the probe beam through the quarter-wave plate, after probing the atoms in the vapor cell, distinguishes POLEAS from PS. This results in the absorption profiles rather than the dispersion profiles, as described in Section 2. This quarter-wave plate, in conjunction with the subsequent PBS, acts as a circular analyzer, measuring the ellipticity of the probe beam. The two components of the probe beam are directed, by the PBS, onto a balanced photodetector that amplifies and subtracts them.

5. Results

The spectra of the ^{87}Rb $F = 2 \rightarrow F'$ hyperfine manifold using the D-F SAS and POLEAS methods

are shown in Fig. 3. The dramatic increase in signal strength for the $F = 2 \rightarrow F' = 3$ cycling resonance is clearly evident. These spectra were obtained with the same input beam parameters (27 μW, 3 mm diameter), and the same magnetically shielded vapor cell, in order to make as fair a comparison as possible. The theoretically predicted spectra are shown in Fig. 3(a), and the experimental results in Fig. 3(b). The agreement between theory and experiment is reasonably good. The slight discrepancies are attributed to residual magnetic fields and the approximately 1 MHz laser linewidth, neither of which were accounted for in the theory.

This enhanced signal-to-noise ratio (S/N) ratio can be leveraged to improve the stability of a laser frequency lock. We locked the frequency of our laser to the $F = 2 \rightarrow F' = 3$ peak using the POLEAS method. This was done by the common phase-sensitive peak-lock method that is often employed with D-F SAS signals. Here, the laser-diode's current is modulated at 10 kHz, and the error signal is filtered using proportional and integral gain. The resulting correction signal is fed back onto the laser current.

To accurately measure the frequency stability of the locked laser it is necessary to compare with a reference oscillator that is well characterized and known to be significantly more stable than the device under test, but such a reference oscillator is not available in our case. Recording a time-series measurement of the error signal allows an Allan deviation [21] to be calculated. This does not necessarily reveal the frequency stability, but it can be indicative. We used this method and found the Allan deviation of our locked laser to be 4×10^{-11} at 1 s, which is approximately two orders of magnitude better than that of the unlocked case. The frequency stability at longer times is limited by environmental sensitivities (see Discussion section below).

The servo loop bandwidth is limited by the 10 kHz modulation signal, and no attempts were made to increase this bandwidth, as we are chiefly concerned with low-frequency gain for a large hold-in range (to maintain lock over long periods). In principle, the bandwidth could be increased up to a significant fraction of the atomic transition linewidth, though applying such high-frequency modulation to the light would require an external optical modulator (such as an acousto-optic or electro-optic modulator). We find the POLEAS method of laser stabilization to be robust and reliable in that the laser remains locked for days, and provides consistent performance for atomic laser cooling experiments.

While the increased signal strength of the cycling resonance is the most striking attribute of the POLEAS method, there are other appealing aspects that could prove equally beneficial. The simplicity of the experimental configuration and the fact that the Doppler background is automatically removed without the need for a separate beam (as in D-F SAS), mean that POLEAS can readily be implemented in a compact package [22]. Furthermore, by enhancing the cycling transition signal and simultaneously reducing the other nearby spectral features, an auto-locking laser stabilization scheme becomes easier to accomplish, especially compared with D-F SAS, where the crossover peaks provide the strongest features. These are two important factors to consider for remote, autonomous, or space-bound systems, such as atomic clocks for satellite navigation.

6. Discussion

The frequency stability of an oscillator is often characterized by its Allan deviation $\sigma(\tau)$ [23]. At short times, assuming white noise only, the Allan deviation is inversely proportional to the signal-to-noise ratio (S/N) of the spectroscopic resonance signal, $\sigma(\tau) \propto (S/N)^{-1}$, [24]. This indicates that the short-term frequency stability of a laser locked to the closed $F = 2 \rightarrow F' = 3$ transition using the POLEAS method can be significantly better than that using the D-F SAS method, since the S/N of POLEAS is much greater than D-F SAS. At longer times, the frequency stability is limited by drifts of the lock point, due to environmental sensitivities of the spectrometer.
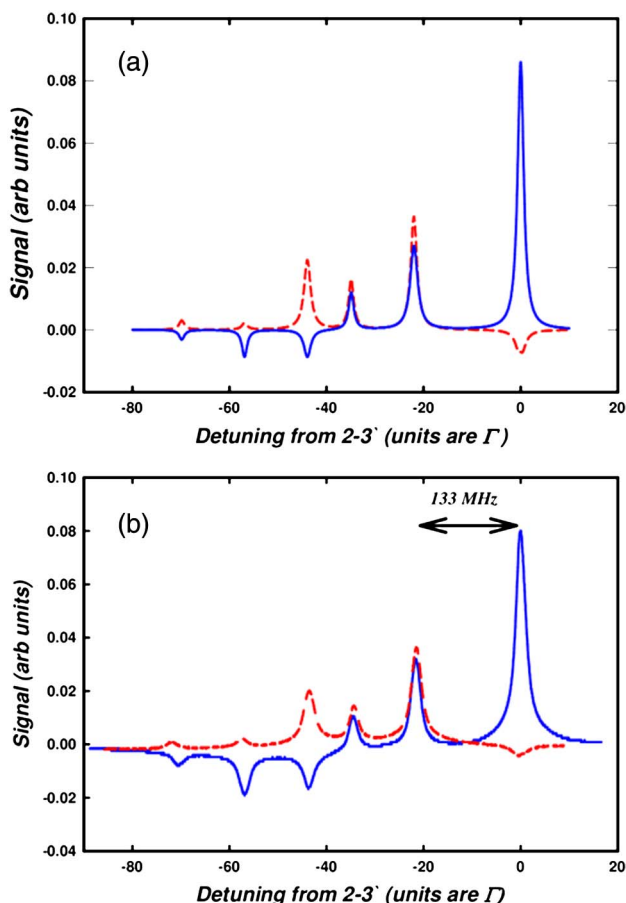

Fig. 3. (a) Theoretically predicted spectra. (b) Experimental data. Dashed line is D-F SAS, and solid line is POLEAS taken under similar conditions. Units are the same for both figures.

Although D-F SAS is routinely used and has demonstrated adequate long-term frequency stability for many atomic physics experiments, PS appears more susceptible to environmental perturbations. Temperature sensitivity in PS has been reported to be a main cause of the observed drift rates of order MHz/hour [7]. Without special attention paid to mitigating these drifts, PS would not provide consistent, day-to-day, long-term frequency stability sufficient for many applications. It should be noted that a more complicated, but related, configuration, termed *bi-polarization spectroscopy* (BPS), has realized reduced drift rates compared with conventional PS [8].

One important difference between the methods, related to temperature sensitivity, is the use of wave plates that are known to be temperature sensitive (of order $10^{-4}(\Delta\lambda/\lambda)/°C$ for zero-order wave plates); where as, D-F SAS typically uses no wave plates, PS typically uses one quarter-wave plate and one half-wave plate, and POLEAS uses a single quarter-wave plate. We measured the dependence of the POLEAS lock-point on the angle of its quarter-wave plate by locking the laser to the POLEAS signal and using the D-F SAS for a frequency discriminator. We rotated the POLEAS quarter-wave plate by ± 5 deg around its nominal 45 deg alignment, and found the frequency-to-angle dependence to be 260 ± 80 kHz/deg, which corresponds to an approximate temperature sensitivity of 104 ± 32 Hz/°C (using the typical temperature coefficient for zero-order plates given above). We set up a PS experiment for comparison, and, although its *quarter-wave* plate demonstrated similar sensitivities, the *half-wave* plate was found to be roughly one hundred times more sensitive. The high sensitivity of the PS lock to its half-wave plate is due to the direct impact that the half-wave plate has on the amplitude balance between the photodetectors of the balanced polarimeter. This half-wave plate is likely a significant contributor to the frequency drifts previously reported with PS laser stabilization.

Another difference between the spectrometers related to temperature sensitivities is that D-F SAS and POLEAS rely on absorption coefficients, while PS relies on birefringence. Reports in the literature have cited temperature-dependent birefringence of cell windows as a vulnerable component, due to the mechanical stresses on the windows from the manufacturing process [7]. The D-F SAS and POLEAS methods have the advantage of relative insensitivity to changes in the windows' birefringence.

Magnetic field sensitivities are another aspect that must be considered when using spectroscopy-based laser stabilization. Generally, magnetic shielding is not used for D-F SAS, but it is for PS and POLEAS. This is because, with D-F SAS we often lock to a crossover peak for greatest S/N, and crossover peaks are visible in the presence of fields typically experienced in the lab. Such visibility is not necessarily true for the $F = 2 \rightarrow F' = 3$ cycling transition. This transition is strongly affected by the mechanisms of optical pumping and atomic polarization, which rely on the relative orientation of the quantization and optical polarization axes and, hence, are sensitive to external fields. In POLEAS and PS, this cycling resonance provides the greatest S/N, and therefore magnetic shielding is desirable for consistent, optimal performance.

The effect that magnetic fields have on the spectrometers' signals depends on their relative orientation. Transverse magnetic fields tend to reduce the atomic spin polarization and, correspondingly, the signal strengths observed with POLEAS and PS. Longitudinal magnetic fields result in a resonant Faraday or Macaluso–Corbino effect [25] that can be observed as a change in the Doppler-broadened background signal, but this has much less impact on the narrow sub-Doppler features. To investigate this we placed the cell in a solenoid, and shielded them both with mu-metal. In this way, we could vary the longitudinal field from 0 to 1500 mG, while keeping the transverse magnetic field less than 4 mG. To measure the POLEAS lock point sensitivity to longitudinal magnetic fields we locked the laser, as usual, to the $F = 2 \rightarrow F' = 3$ cycling peak and used the D-F SAS as a frequency discriminator. We observed no measurable change in the lock frequency when ramping the longitudinal magnetic field from 0 to 1500 mG. In fact, with the solenoid providing a longitudinal field of 750 mG, we could forego the mu-metal shield and yet the amplitude of the cycling peak remained with 88% of its shielded value (without the shield the transverse magnetic field varied over the length of the cell, but was everywhere less than 400 mG). Furthermore, as a very crude test, we observed that, by placing a small permanent bar magnet (aligned longitudinally) near the cell, neither the solenoid, nor the mu-metal shield was needed. In this case, the longitudinal magnetic field varied from 150 to 500 mG over the length of the cell; nevertheless, the amplitude of the cycling peak was 67% of its shielded value. This indicates that the POLEAS method can be used without expensive magnetic shielding.

7. Conclusion

We have demonstrated a variation of pump-probe spectroscopy that is particularly useful for laser frequency stabilization. The polarization enhanced absorption spectroscopy (POLEAS) signals provide a significant improvement in S/N over standard D-F SAS for the important and commonly used $F = 2 \rightarrow F' = 3$ cycling transition. This improvement can directly increase the short-term stability of a laser frequency-lock, given sufficient loop bandwidth. The long-term stability of the POLEAS method is comparable to D-F SAS, and significantly better than standard PS. The POLEAS signal is automatically Doppler-free, without requiring a separate Doppler subtraction beam, and lends itself to straightforward

compact packaging. Finally, by increasing the amplitude of the desired (cycling) peak while reducing the amplitude of all other peaks in the manifold, the POLEAS method eases the implementation of auto-relocking schemes.

References

1. T. Kessler, C. Hagemann, C. Grebing, T. Legero, U. Sterr, F. Riehle, M. J. Martin, L. Chen, and J. Ye, "A sub-40-mHz-linewidth laser based on a silicon single-crystal optical cavity," Nat. Photonics **6**, 687–692 (2012).
2. W. Demtröder, *Laser Spectroscopy* (Springer, 2008).
3. K. B. MacAdam, A. Steinbach, and C. Wieman, "A narrowband tunable diode laser system with grating feedback, and a saturated absorption spectrometer for Cs and Rb," Am. J. Phys. **60**, 1098–1111 (1992).
4. O. Schmidt, K.-M. Knaak, R. Wynands, and D. Meschede, "Cesium saturation spectroscopy revisited: how to reverse peaks and observe narrow resonances," Appl. Phys. B **59**, 167–178 (1994).
5. C. Wieman and T. W. Hänsch, "Doppler-free laser polarization spectroscopy," Phys. Rev. Lett. **36**, 1170–1173 (1976).
6. C. P. Pearman, C. S. Adams, S. G. Cox, P. F. Griffin, D. A. Smith, and I. G. Hughes, "Polarization spectroscopy of a closed atomic transition: applications to laser frequency locking," J. Phys. B **35**, 5141–5151 (2002).
7. Y. Yoshikawa, T. Umeki, T. Mukae, Y. Torii, and T. Kuga, "Frequency stabilization of a laser diode with use of light-induced birefringence in an atomic vapor," Appl. Opt. **42**, 6645–6649 (2003).
8. V. B. Tiwari, S. Singh, S. R. Mishra, H. S. Rawat, and S. C. Mehendale, "Laser frequency stabilization using Doppler-free bi-polarization spectroscopy," Opt. Commun. **263**, 249–255 (2006).
9. T. Wu, X. Peng, W. Gong, Y. Zhan, Z. Lin, B. Luo, and H. Guo, "Observation and optimization of ^{4}He atomic polarization spectroscopy," Opt. Lett. **38**, 986–988 (2013).
10. C. Javaux, I. G. Hughes, G. Lochead, J. Millen, and M. P. A. Jones, "Modulation-free pump-probe spectroscopy of strontium atoms," Eur. Phys. J. D **57**, 151–154 (2010).
11. P. Kulatunga, H. C. Busch, L. R. Andrews, and C. I. Sukenik, "Two-color polarization spectroscopy of rubidium," Opt. Commun. **285**, 2851–2853 (2012).
12. C. Carr, C. S. Adams, and K. J. Weatherill, "Polarization spectroscopy of an excited state transition," Opt. Lett. **37**, 118–120 (2012).
13. V. V. Yashchuk, D. Budker, and J. R. Davis, "Laser frequency stabilization using linear magneto-optics," Rev. Sci. Instrum. **71**, 341–346 (2000).
14. H.-R. Noh, G. Moon, and W. Jhe, "Discrimination of the effects of saturation and optical pumping in velocity-dependent pump-probe spectroscopy of rubidium: a simple analytical study," Phys. Rev. **82**, 062517 (2010).
15. G. Moon and H. R. Noh, "A comparison of the dependence of saturated absorption signals on pump beam diameter and intensity," J. Opt. Soc. Am. B **25**, 2101–2106 (2008).
16. G. Moon, M.-S. Heo, S. R. Shin, H.-R. Noh, and W. Jhe, "Calculation of analytic populations for a multilevel atom at low laser intensity," Phys. Rev. **78**, 015404 (2008).
17. G. Moon and H.-R. Noh, "Analytic calculation of linear susceptibility in velocity-dependent pump-probe spectroscopy," Phys. Rev. **78**, 032506 (2008).
18. H. D. Do, G. Moon, and H.-R. Noh, "Polarization spectroscopy of rubidium atoms: theory and experiment," Phys. Rev. **77**, 032513 (2008).
19. G. Moon and H. R. Noh, "Analytic solutions for the saturated absorption spectra," J. Opt. Soc. Am. B **25**, 701–711 (2008).
20. D. A. Smith and I. G. Hughes, "The role of hyperfine pumping in multilevel systems exhibiting saturated absorption," Am. J. Phys. **72**, 631–637 (2004).
21. D. W. Allan, "Statistics of atomic frequency standards," Proc. IEEE **54**, 221–230 (1966).
22. D. Groswasser, A. Waxman, M. Givon, G. Aviv, Y. Japha, M. Keil, and R. Folman, "Retroreflecting polarization spectroscopy enabling miniaturization," Rev. Sci. Instrum. **80**, 093103 (2009).
23. L. D. Turner, K. P. Weber, C. J. Hawthorn, and R. E. Scholten, "Frequency noise characterization of narrow linewidth diode lasers," Opt. Commun. **201**, 391–397 (2002).
24. H. Talvitie, M. Merimaa, and E. Ikonen, "Frequency stabilization of a diode laser to Doppler-free spectrum of molecular iodine at 633 nm," Opt. Commun. **152**, 182–188 (1998).
25. D. Budker, W. Gawlik, D. F. Kimball, S. M. Rochester, V. V. Yashchuk, and A. Weis, "Resonant nonlinear magneto-optical effects in atoms," Rev. Mod. Phys. **74**, 1153–1201 (2002).